Measured Performance and CST-Based Analysis of Compact UWB Vivaldi Antenna for Wind Turbine Blade Health Monitoring

Sahar Saleh[1,2], Tale Saeidi[1], Qusay Shihab Hamad[3], Nick Timmons[1], Farooq Razaz[4], Shahanawaz Kamal[5]
[1] WiSAR Lab, Atlantic Technological University (ATU), Letterkenny, Co. Donegal, F92 YY97, Ireland, sahar.saleh@atu.ie*, tale.saeidi@atu.ie, nick.timmons@atu.ie
[2] University of Aden, Aden, Yemen, sahar.abdulrazzaq.eng@aden-univ.net
[3]University of Information Technology and Communications (UoITC), Baghdad, Iraq,qusay.phd@gmail.com
[4]Electrical Engineering Department, Prince Sattam Bin Abdulaziz University, Al-Kharj, Saudi Arabia, f.kasim@psau.edu.sa
[5]Radio Frequency Design Enablement Group, Barkhausen Institut, Dresden, Germany, shahanawaz.kamal@barkhauseninstitut.org

***Abstract*— A compact Ultra-Wideband (UWB) Vivaldi Tapered Slot Antenna with Radial Transition (VTSAR) is proposed in this work for applications including structural health monitoring (SHM). The antenna makes notable improvements in size, bandwidth (BW), and gain without the need for additional matching circuits by replacing a radial-to-radial design for the circular-to-circular microstrip-to-slotline transition. Simulations and experiments confirm that the proposed VTSAR has a stable group delay of 1 ns, a wide operational BW of 3.29–17.55 GHz, and stable radiation properties. Using CST simulations with a 3D wind turbine blade model, the antenna is used to detect defects in the blade to illustrate its sensing capabilities. GFRP epoxy, according to material analysis, offers the best performance retention, and results show that the transmission coefficient (S21) of damaged and healthy blades differs noticeably. According to these findings, the VTSAR is a viable and affordable option for accurate UWB sensing and SHM.**

Index Terms*— *Vivaldi Tapered Slot Antenna (VTSA), Ultra-Wideband (UWB), Structural health monitoring (SHM), Wind Turbine Blade (WTB) and CST.

I. INTRODUCTION

Due to its low cost, high data rate, small size, and low power consumption, ultra-wideband (UWB) wireless communication offers great opportunities in the current wireless communication system [1].

Owing to its end-fire symmetrical radiation pattern, broad bandwidth (BW), simple structure, low profile, low production cost, low power consumption, and simplified interface with other circuits, Vivaldi Tapered Slot Antenna (VTSA) is best for UWB technology. Many approaches are proposed to improve its performance [2]. Compactness can be achieved by adding parasites to the radiation patches [3], modify microstrip to slot (M/S) transition [4], using Fan-shaped flare [5], and using Vivaldi non-uniform slot profile antenna (VNSPA) theory [6]. While performance can be improved by adding cavities with slots [7], corrugations [8], [9], [10], [11], stepped slots [5], adding metamaterial (MTM), [10] using VNSPA theory [6] and using grating elements [9], [11], [12].

Infrastructure safety requires structural health monitoring (SHM). Visual inspections, X-rays, and ultrasonic testing are dependable and accurate, but they are expensive, require several sensor arrays, and make data administration difficult. Indirect detection, which uses fewer sensors to detect minor deflections like stiffness or damping, is cheaper but less reliable. In wind energy, where maintenance costs account for 40% of operational costs, SHM must balance cost and performance to reduce downtime Strain gauges, acoustic emission sensors, and fiber optics monitor wind turbines efficiently. However, accessibility (particularly in offshore farms), detaching sensors due to adverse weather, and high costs are issues. As an alternative, wireless sensor networks (WSNs) are used, which include transducers, signal conditioning circuits, and processing software. They caused high sampling rates and synchronization; however, improved digital signal processing (DSP) can reduce this. RF radars with diverse antenna types and frequency bands have solved the prior detection methodology issues and provided high-accuracy detection [13], [14].

Studies in [15], [16] employed UWB antennas along the blade's tip and root to identify wind turbine bending deflection by calculating the pluses' arrival times. However, a 79 GHz FMCW radar on top of the blade tower was used to detect tower collisions in [17]. Polarization-based (circular) microstrip arrays are used to enhance the signal-to-noise ratio (SNR) and reduce interference. The transmitting channel is combined into one to focus power to the tip and have a focused angle instead of azimuth resolution. Based on EMPIRE XPU 8.01 numerical modelling studies, a single transmitter-receiver pair can accurately identify cracks in small specimens and full-scale blades by distorting the electric field signal [18]. Cracks were found regardless of depth. After using solely electric field data, integrating magnetic field data with elastic wave modelling using an antipodal Vivaldi antenna improves crack location and characterization.

Inspired by [15], [16], in this work, we are placing two UWB VTSA with radial transition (VTSAR) antennas on the tip and root of a small wind turbine blade (WTB) imported to

978-88-31299-12-1/26/$31.00 ©2026 IEEE

CST to detect blade tip deflection and cracks. The effect of blade material on antenna performance is also investigated. To the authors' knowledge, this is the first CST-based study examining material-dependent UWB signal propagation along turbine blades, enabling reliable laboratory evaluation while reducing the cost associated with testing and recycling large blades that may crack during operation [18]. This study prepares the groundwork for defect identification utilizing mmWave FMCW radar with high-performance and efficient antennas intended for field measurement.

In addition to this section, Section II discusses the VTSAR design, while Section III presents the analysis of the proposed antennas on WTB using CST. Section IV discusses the results. Finally, Section V concludes the work.

II. Antenna Design: VTSAR

Figure 1(a) illustrates the layout of the proposed VTSAR antenna, which is obtained by replacing the circular-to-circular microstrip-to-slot (M/S) transition in VTSA [4] with a radial-to-radial transition to enhance BW and gain while maintaining a compact size. Rogers RO4003C substrate (εr = 3.55, h = 0.813 mm) is used in designing the VTSAR. In Fig. 1(a), the dimensions, W_{min} = 0.3 mm, W_{max} = 21.03 mm, L_{qw} = 4.6 mm, *radsl*= 2 mm, *angsl*, = 150°, *angst*= 120°, L_T = 25 mm, L_f = 18.3 mm, W_f = 1.25 mm, W_{ant}= 39.6 mm, and L_{ant} = 28.6 mm are the opening width, opening aperture, quarter-wave slot length, radius of slot, angle of slot, angle of stub, taper slot length, feeding length, feeding width, antenna width and antenna length, respectively. *dis* is the distance between L_{ant} and L_{qw} =L_{ant} - L_{qw} = 35 mm. These optimized values obtained using parametric studies shown in Fig. 2. The other parameters, which are not shown in the figure, were obtained from the VTSA in [4]. The fabricated VTSAR is shown in Fig. 1(b) as compared to the VTSA [4].

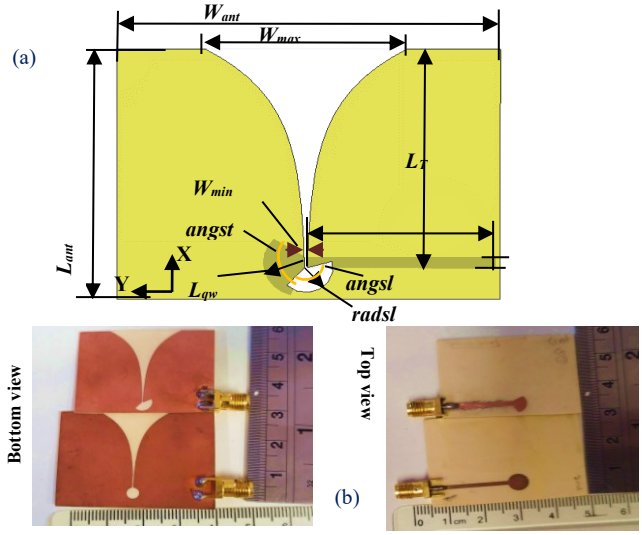

Fig. 1. (a) Layout of the proposed compact UWB VTSAR and (b) its prototype as compared to VTSA [4].

A one-at-a-time parametric analysis was performed to assess the impact of key geometric parameters on impedance matching and BW. This analysis is used to determine the optimal configuration, balancing BW, realized gain, and antenna size. While all parameters influence the antenna response, L_{qw} and *radsl* show the strongest sensitivity due to their direct role in the microstrip-to-slot transition, whereas the remaining parameters mainly provide fine-tuning of bandwidth and impedance smoothness. The optimized VTSAR achieves wide BW, low S_{11}, and high realized gain suitable for placement along wind turbine blades (WTBs). With a maximum realized gain of 7.19 dBi and an area of 1132.56 mm^2, the best result for UWB VTSAR providing S_{11} <-11.37 dB at 3.29 –17.55 GHz was obtained at the optimized parameters indicated by the red solid line in Fig. 2. The obtained area is 11.41% reduced as compared to VTSA in [4].

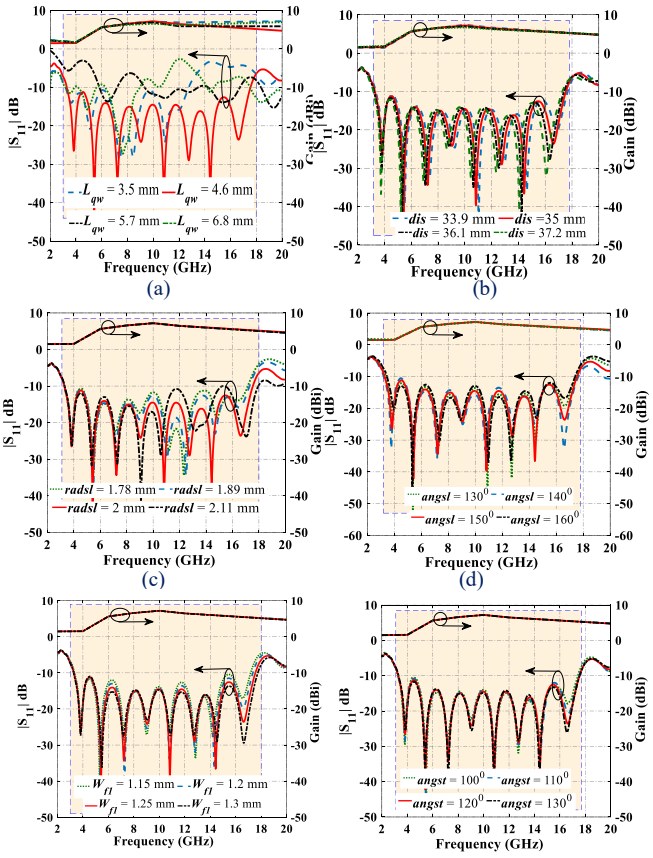

Fig. 2. S_{11} and gain parametric study of the proposed compact UWB Antenna 1 on (a) L_{qw}, (b) *dis*, (c) *radsl*, (d) *angsl*, (e) *angst*, and (f) W_{fl}

III. Wind Turbine Blade Deflection Application

Since the wind turbine blade acts as a nearby dielectric and lossy structure, its material properties influence the electromagnetic loading and performance of blade-mounted antennas. So, they should be taken into consideration for improved monitoring. For this purpose, we investigate this effect on the antenna performance in terms of S11, S21, and Group delay (GD), and compare them to the free space case. This is considered a reliable baseline for subsequent blade-deflection and crack-detection analysis, where differential changes relative to this reference will be the primary indicators of structural anomalies. A 3D CAD model of a healthy (crack-free) WTB was imported into CST. An exterior

shell layer is used to represent the blade for parametric analysis, capturing the dominant electromagnetic interaction between the blade and the surface-mounted antennas while reducing computational complexity. Internal structural components and multilayer composite effects are not considered at this stage and will be investigated in future work. Following the study in [15], [16], two identical VTSAR antennas are positioned at the tip and root of the blade, as shown in Fig. 3(a). Antennas embedded in blades may provide extra protection and regulated electromagnetic propagation; however, they are highly dependent on blade manufacturing processes and material layup, which will be considered in future investigations. This work presents a compact polycarbonate (in blue color) radome with rounded edges to protect the proposed VTSAR from environmental exposure and blade vibrations. Polycarbonate is selected due to its mechanical robustness, low moisture absorption, and stable dielectric properties under outdoor operating conditions [19]. Different blade materials in CST were defined by their permittivity (εr) and loss tangent (tanδ) and listed in Table I. PETG (Polyethylene Terephthalate Glycol-modified) material is added due to its closet characteristics to the blade materials, facilitating the fabrication of a small prototype in the lab later on a 3D printer (e.g., Bambu Labs X1E) for testing the antenna's performance in detecting wind blade cracks using the PNA.

Figure 3(b) shows the absolute reflection coefficient (S_{11}) of the proposed antenna for all investigated materials. Compared to free-space, the antenna maintains good impedance matching when mounted on the blade, confirming its suitability for SHM measurements. In particular, GFRP-based composites exhibit smooth and stable S_{11} behavior without excessive resonances, indicating reliable antenna–material coupling and repeatable operating conditions. Material selection is therefore based on transmission and propagation characteristics. As shown in Fig. 3(c-e), GFRP epoxy demonstrates moderate attenuation S_{21} (Fig. 3(c)), smooth and repeatable ΔS_{21} behavior (Fig. 3(d)), and the most stable GD (Fig. 3(e)) among the candidates. These features establish a robust electromagnetic baseline that is essential for detecting small damage-induced perturbations. Thermoplastic and recyclable composites are also promising option for future sustainability-oriented designs. Natural fiber composites can serve as a proof-of-concept material but are less ideal mechanically. In contrast, CFRP is too lossy, causing signal collapse that masks crack detection, while PETG is overly EM-transparent, resulting in insufficient sensitivity. Consequently, GFRP epoxy is selected for crack and deflection detection in the next section. This explains why GFRP-based composites are the preferred material in RF-SHM studies and motivates their use as the primary platform in this work [20].

TABLE I: ELECTRIC PROPERTIES FOR DIFFERENT BLADE MATERIALS

Material	ε_r	***tanδ***
GFRP Epoxy	4.7	0.02
CFRP Epoxy(effective isotropic)	11.0	0.015
GFRP Polyester	4.5	0.025
High-Strength Carbon Fiber Composites	3.5	0.015
Natural Fiber Composites	3.2	0.025
PETG	2.4	0.02
Thermoplastic Composites	3	0.02
Smart Materials	4	0.02
Recyclable-by-Design Materials	3.2	0.02

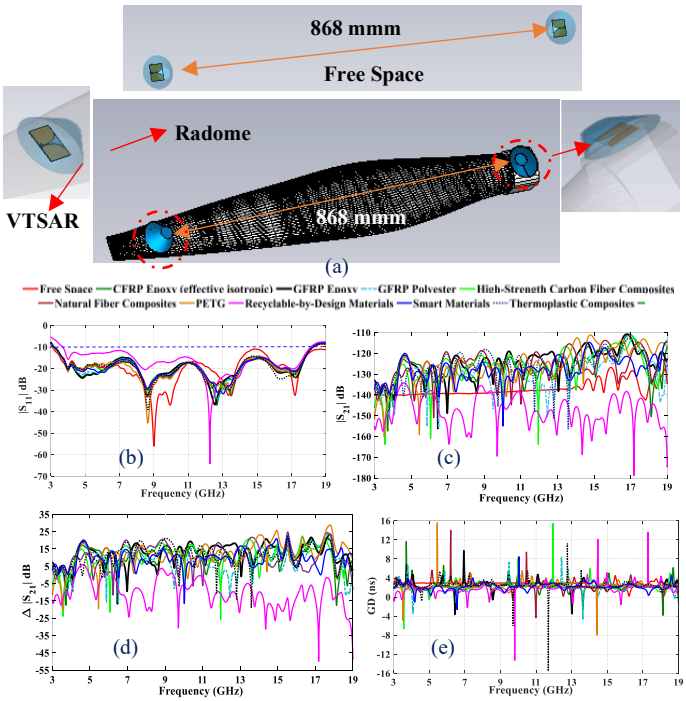

Fig. 3. (a) The two VTSAR on free space and healthy WBT on CST, (b) the resulting simulated S_{11} =S_{22} and (b)S_{21} using different blade materials.

IV. RESULTS AND DISCUSSION

This section compares the proposed VTSAR's results to VTSA in [4] and demonstrates VTSAR's capability to identify cracks and deflectionon the WBT. Simulated and measured antenna performance data provide a complete picture and validate the proposed methods. Analyses of impedance bandwidth, gain, radiation patterns, and GD demonstrate the designs' appropriateness for modern applications. Note that these measurements were performed in free space to validate standalone antenna performance; interactions with a WTB and practical SHM operation will be explored in future work using a PETG prototype. As shown in Fig. 4, the proposed compact UWB VTSAR achieves a good, measured matching of < -11.13 dB (from 3.29 to 18.21 GHz) and maximum realized gain (MRG) of 7.2 dBi, with a 30.70% wider BW, 27.78% increased gain, and 11.41% size reduction compared to the designed VTSA in [4] (S_{11} <-11.15 at 3.14-13.48 GHz with MRG of 6.51 dBi). Figure 4(b) shows that VTSAR's total radiation efficiency is 65%–94.08%. In Fig. 5, the end fire and dipole E and H plane radiation patterns show VTSAR's directional property. Finally, Fig. 6 demonstrates that VTSAR has a steady group delay of 1 ns (Sim. = 0.75 ns) across the BW. These results prove that the parametric studies and the radial transition can reduce VTSA size and increase BW and gain without adding matching circuits or parasites. The BW and gain of this optimized

antenna are enhanced by 31.95 % and 7.78 %, respectively, and the size is reduced by 9.84 % as compared to VTSA [4] (S_{11} <-10.84 at 2.95-12.79 GHz with MRG of 6.63 dBi and area of 1256.112 mm^2).

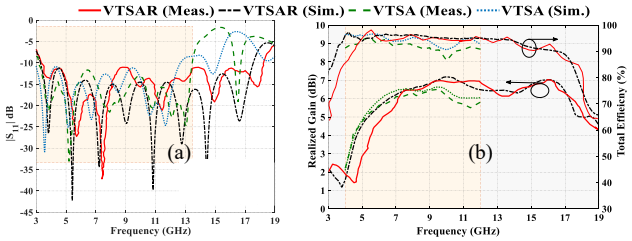

Fig. 4. Simulated and measured (a) S_{11} and (b) gain with total radiation efficiency of compact UWB VTSAR as compared to VTSA in [4]

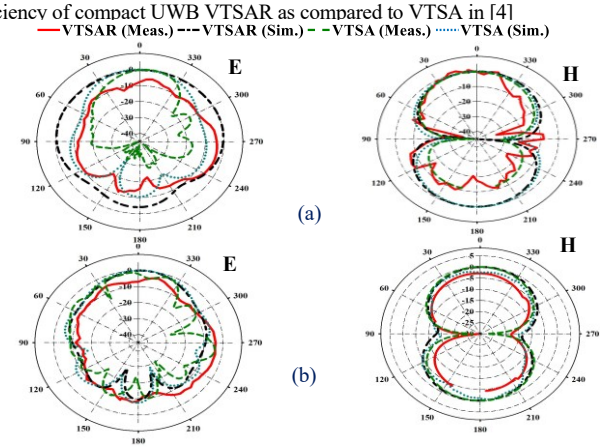

Fig. 5. Simulated and measured radiation patterns of compact UWB VTSAR as compared to VTSA in [4] at (a) F= 5.11 GHz and (b) F= 10GHz

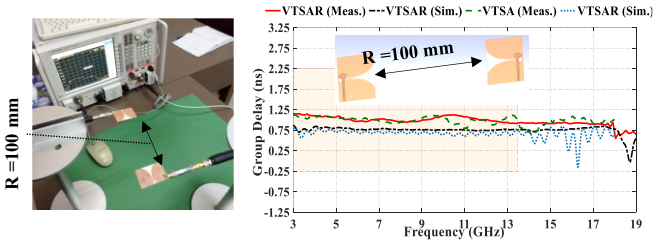

Fig. 6. Simulated and measured group delay of compact UWB VTSAR as compared to VTSA in [16] with measurement and simulation setup

Finally, the influence of both structural damage and blade deformation on reflection coefficient (S_{11} = S_{22}) and transmission coefficient (S_{21}) of the two antennas mounted on the GFRP epoxy-based blade is investigated as illustrated in Fig. 7. In addition to crack scenarios at the blade center and edge shown in Fig. 7(a-b), tip deflection which is commonly experienced by wind turbine blades under wind loading is considered by applying tip bending (normal and severe bending) as shown in (Fig. 7(c)). As shown in Fig. 3(d), the S_{11} exhibits only minor variations with crack location and blade deflection, while the overall impedance matching remains stable, indicating robust antenna operation under structural damage and deformation. However, the S_{21} in Fig. 7(e) exhibits clear and measurable variations for center and edge cracks, as well as for moderate and severe tip deflection. Crack-induced perturbations are more pronounced for center cracks, while deflection produces smooth, broadband changes with increasing magnitude. These results confirm that S_{21} is the primary indicator for crack and deflection detection, whereas S_{11} serves to validate antenna robustness under realistic operating conditions.

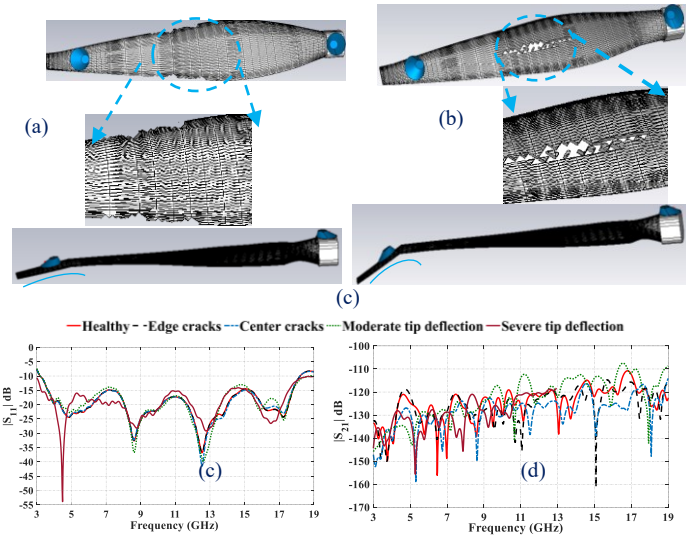

Fig. 7. blade with (a) edge crak, (b) center crack, (c) tip deflection , (d)S_{11}, and (e) S_{21}.

Table II compares the proposed UWB VTSAR with recently reported antennas employing different M/S techniques, showing that the proposed radial-to-radial M/S transition achieves superior impedance bandwidth while maintaining compact size and low design complexity. Although the antennas in [6] and [21], based on VNSPA theory, achieve smaller physical sizes, the proposed design outperforms them in terms of BW and realized gain due to the adopted transition approach; the integration of VNSPA theory with the proposed VTSAR will be explored in future work. Compared with [4], replacing the circular transition with radial one results in a 30.70% wider bandwidth, a 27.78% increase in realized gain, and 11.41% size reduction.

TABLE II: COMPARISON OF THE PROPOSED VTSAR WITH STATE-OF-THE-ART ANTENNAS

Ref.	ε_r	S_{11}(dB) at Freq. Band (GHz), BW	MG (dBi)	C or E techniques	Feeding M/S:	Volume mm × mm × mm
This work	**3.55**	**<-11.13 at 3.29 –17.55,**	**1.7 – 7.2**	——	**Radial/ Radial**	**39.6 × 28.6 × 0.813**
[6]		<-11.36 at 2.63 – 12.33,9.7	2 – 5.9		Circular/ Circular	23.2 × 14.76 × 0.813
Antenna A [21]		<-10.21 at 3.16 – 14.34,11.18	1.9 – 6			19.22 × 12.368× 0.813
Antenna B [21]		<-10.89 at 2.9– 13.55,10.65	1.8-6.91			29.8 × 20.26 × 0.813
VTSA [4]		<-11.15 at 3.14 – 13.48,10.34	2.2-6.51			42.9 × 29.28 × 0.813
[8]	4.4	<-10 at 3.2 – 16.8, 13.6	5 – 10.4	Corrugations	Circular/ Circular	34 × 33 × 0.80
[5]	3.5	<-10 at 2.32– 13.75, 11.43	3.1–7.9	Fan-shaped and stepped structures	Circular/ Circular	36 × 36 × 0.76
[9]	4.2-4.8	< -10 at 3–8	7.2 – 8.75	Corrugations & metal strips	Rectangle/ Rectangle	110 × 96× 0.8
[11]	4.3	< -10.4 at 1.1– 8	4.9 – 10	Corrugations and director	M/S: Radial / Circular	82 × 55× 1.6
[10]	2.2	< -11.14 at 2– 11.79	0– 7.9	Side slots and MTM		40×46×1.575

Furthermore, the proposed antenna is smaller than those reported in [5], [8], [10], [11], [12] while achieving a wider BW without additional components. The higher gains reported in these works are mainly attributed to larger antenna sizes and added performance-enhancement techniques, which increase design complexity compared to the proposed antenna.

I. CONCLUSION

A simple M/S transition to radial/radial can improve the compactness and performance of the UWB VTSAR, as shown in this work. VTSAR outperformed VTSA in size, BW, and gain by 9.84%, 31.95%, and 7.78%, respectively, without matching circuits. The proposed VTSAR's simulated and observed findings indicate its wide BW (3.29 –17.55 GHz), steady GD (1 ns), and stable radiation features. These properties make the antenna perfect for UWB sensing, which is used to identify wind turbine blade problems. In CST, an imported 3D blade is utilized to evaluate the influence of different blade materials on the electromagnetic response of antennas mounted at the blade root and tip. Based on S-parameter and GD analysis in the healthy state, GFRP epoxy is identified as the most suitable material, offering a favorable trade-off between electromagnetic transparency, stability, and mechanical relevance. Subsequently, structural damage and operational deformation are examined by introducing cracks at different blade locations and applying moderate and severe blade tip deflection. While both effects introduce only minor variations in the antenna reflection coefficient (S_{11}), overall impedance matching remains stable; in contrast, clear and consistent variations are observed in the transmission coefficient (S_{21}), confirming its suitability for detecting crack- and deflection-induced perturbations. These findings inform future flaw detection research and make UWB VTSAR a promising candidate for WBT monitoring at low cost. Experimental validation using a small PETG wind turbine blade with controlled cracks, defect type and severity characterization, and application to larger blades in real operations are planned. We will investigate hybrid sensing systems employing UWB antennas with mmWave FMCW radar or machine learning to improve the deflection localization and classification.

REFERENCES

[1] V. Zhurbenko, Passive microwave components and antennas. BoD–Books on Demand, 2010.

[2] S. Saleh, T. Saeidi, N. Timmons, and F. Razzaz, "A comprehensive review of recent methods for compactness and performance enhancement in 5G and 6G wearable antennas," Alexandria Engineering Journal, vol. 95, pp. 132–163, May 2024, doi: 10.1016/J.AEJ.2024.03.097.

[3] T. Yang, D. Yang, B. Wang, and J. Hu, "Experimentally validated, wideband, compact, OAM antennas based on circular vivaldi antenna array," Progress In Electromagnetics Research C, vol. 80, no. January, pp. 211–219, 2018, doi: 10.2528/pierc17110702.

[4] S. Saleh, W. Ismail, I. S. Z. Abidin, M. H. Jamaluddin, M. H. Bataineh, and A. S. Alzoubi, "Compact UWB Vivaldi Tapered Slot Antenna," Alexandria Engineering Journal, vol. 61, no. 6, pp. 4977–4994, 2022, doi: 10.1016/j.aej.2021.09.055.

[5] J. Yeo and J. I. Lee, "Compact Wideband Tapered Slot Antenna Using Fan-Shaped and Stepped Structures for Chipless Radio-Frequency-Identification Sensor Tag Applications," Sensors, vol. 24, no. 12, Jun. 2024, doi: 10.3390/s24123835.

[6] S. Saleh, W. Ismail, I. S. Zainal Abidin, M. H. Jamaluddin, M. H. Bataineh, and A. S. Al-Zoubi, "Novel Compact UWB Vivaldi Nonuniform Slot Antenna With Enhanced Bandwidth," IEEE Trans Antennas Propag, vol. 70, no. 8, pp. 6592–6603, 2022, doi: 10.1109/TAP.2022.3161281.

[7] Z. Tahar, X. Dérobert, and M. Benslama, "An Ultra-Wideband Modified Vivaldi Antenna Applied to through the Ground and Wall Imaging," Progress In Electromagnetics Research, vol. 86, pp. 111–122, 2018.

[8] H. Zhang and F. Zhang, "A Novel Ultra-wideband Miniature Vivaldi Antenna with Sawtooth Outer Edges and Inclined Elliptical Slots," IEEE Antennas Wirel Propag Lett, 2024, doi: 10.1109/LAWP.2024.3405007.

[9] J. Wang, J. Liu, Y. Fan, and Y. Bai, "A novel Vivaldi antenna for UWB detection," Microw Opt Technol Lett, vol. 65, no. 3, pp. 826–843, Mar. 2023, doi: 10.1002/mop.33551.

[10] M. T. Islam, M. T. Islam, M. Samsuzzaman, H. Arshad, and H. Rmili, "Metamaterial loaded nine high gain vivaldi antennas array for microwave breast imaging application," IEEE Access, vol. 8, pp. 227678–227689, 2020.

[11] J. Ren, H. Fan, Q. Tang, Z. Yu, Y. Xiao, and X. Zhou, "An Ultra-Wideband Vivaldi Antenna System for Long-Distance Electromagnetic Detection," Applied Sciences (Switzerland), vol. 12, no. 1, 2022, doi: 10.3390/app12010528.

[12] N. Nurhayati, E. Setijadi, A. M. de Oliveira, D. Kurniawan, and M. N. M. Yasin, "Design of 1 × 2 MIMO Palm Tree Coplanar Vivaldi Antenna in the E-Plane with Different Patch Structure," Electronics (Switzerland), vol. 12, no. 1, Jan. 2023, doi: 10.3390/electronics12010177.

[13] A. Soumya, C. Krishna Mohan, and L. R. Cenkeramaddi, "Recent Advances in mmWave-Radar-Based Sensing, Its Applications, and Machine Learning Techniques: A Review," Nov. 01, 2023. doi: 10.3390/s23218901.

[14] S. Saleh, T. Saeidi, N. Timmons, F. Razzaz, and Q. S. Hamad, "Overview of RF-based structural health monitoring of wind turbine blades," Frontiers in Antennas and Propagation, vol. 3, Jan. 2026, doi: 10.3389/fanpr.2025.1755037.

[15] S. Zhang, O. Franek, C. Byskov, and G. F. Pedersen, "Antenna Gain Impact on UWB Wind Turbine Blade Deflection Sensing," IEEE Access, vol. 6, pp. 20497–20505, Mar. 2018, doi: 10.1109/ACCESS.2018.2819880.

[16] O. Franek, S. Zhang, K. Olesen, C. F. Patrick Eggers, C. Byskov, and G. F. Pedersen, "Wind Turbine Blade Deflection Sensing Using Blade-Mounted Ultrawideband Antennas," in 14th European Conference on Antennas and Propagation, EuCAP 2020, Institute of Electrical and Electronics Engineers Inc., Mar. 2020. doi: 10.23919/EuCAP48036.2020.9136004.

[17] J. Chen et al., "A Circularly Polarized Millimeter Wave Radar for Wind Turbine Sensing," Electronics (Basel), vol. 13, no. 2, Jan. 2024, doi: 10.3390/electronics13020462.

[18] Z. R. S. Al-Yasiri, H. M. Mutashar, K. Gürlebeck, and T. Lahmer, "Damage Sensitive Signals for the Assessment of the Conditions of Wind Turbine Rotor Blades Using Electromagnetic Waves," Infrastructures (Basel), vol. 7, no. 8, Aug. 2022, doi: 10.3390/infrastructures7080104.

[19] S. Saleh, T. Saeidi, N. Timmons, A. A. Althuwayb, and F. Razzaz, "Compact 5 G mmWave vivaldi antenna for vehicular communication," Vehicular Communications, vol. 53, Jun. 2025, doi: 10.1016/j.vehcom.2025.100893.

[20] M. E. Rao, J. Moll, P. Kraemer, and V. Krozer, "Experimental Application of a Reversible Reference Damage Model for Radar-Based SHM of Glass Fiber Reinforced Polymer Structures," in 2025 IEEE International Workshop on Metrology for AeroSpace, MetroAeroSpace 2025 - Proceedings, Institute of Electrical and Electronics Engineers Inc., 2025, pp. 780–784. doi: 10.1109/MetroAeroSpace64938.2025.11114561.

[21] S. Saleh, T. Saeidi, N. Timmons, F. Razzaz, and A. A. Althuwayb, "Low SAR ultra compact UWB vivaldi non-uniform slot antennas for breast cancer detection," Phys Scr, vol. 99, no. 12, p. 125541, Nov. 2024, doi: 10.1088/1402-4896/ad9089.